

Comparison of Methods to Detect Thermomechanical Ageing of the Insulation System for Rotating High-Voltage Machines

Lena Elspaß, Stephan Schlegel

*Institute of Electrical Power Systems and High Voltage Engineering, Technische Universität Dresden
Dresden, Germany
lena.elspass@tu-dresden.de*

Hans Bärnklaus

*VEM Sachsenwerk GmbH
Dresden, Germany*

Abstract Increased dynamic operation of long rotating high-voltage machines as well as elevated operating temperatures lead to intensified thermomechanical stress in the insulation system of global vacuum-pressure-impregnated machines. Meanwhile, the requirements regarding reliability of the machine and the electric insulation system remain high. Consequences of thermomechanical stress include delaminations and abrasion. To satisfy the high standards of longevity, reliable diagnosis of thermomechanical ageing is essential to allow manufacturers to develop and improve countermeasures. This work identifies diagnostic tools, which investigate the effects of thermomechanical ageing on model replicates of machine insulation systems. The longitudinal thermal expansion of the conductor during dynamic operation is replicated by applying mechanical force to the conductor of specimens, thus inducing mechanical stress in the insulation system. Recurring measurements of partial discharges, dielectric losses and capacitance are evaluated regarding their sensitivity in detecting resulting ageing phenomena. The study reveals that partial discharge measurements detect preliminary damages before insulation rupture caused by mechanical stress occurs. Knowledge of these capabilities enables future-oriented development of insulation systems for dynamically-operated long rotating machines.

1. Introduction

Rotating high-voltage machines play an important role as generators and drives in our energy system. Longevity of the electrical insulation system is crucial for reliable operation of the machines over decades. Trends towards higher coil temperatures and increasingly dynamic operation lead to higher thermomechanical stress in the insulation system. This ageing mechanism is pronounced in machines manufactured by global vacuum-pressure-impregnation (GVPI) and aggravated by longer coils [1]. Possible results without countermeasures are delaminations, crack formation and abrasion, potentially accelerating the ageing of the insulation. This work investigates diagnostic tools including partial discharge (PD), dielectric loss and capacitance measurements

regarding their ability to detect named ageing phenomena. Scaled-down GVPI-manufactured specimens with an insulated conductor in a slot model are stressed mechanically to replicate longitudinal thermal expansion and thus resulting ageing phenomena. A comparison of various diagnostic tools regarding their ability to detect thermomechanical ageing is given. The results can be applied later on to thermomechanically-aged full-scale test objects, allowing reliable diagnosis and thus future-oriented development of insulation systems for dynamically-operated long rotating machines.

2. State of the Art

Rotating electric machines have to endure several kinds of stress generally known as the TEAM-stresses, comprising thermal, electrical, ambient and mechanical stress. For long machines the combined thermomechanical stress is especially pronounced [1]. For a better understanding of the resulting thermomechanical ageing and the consequences on GVPI insulation systems a short introduction to the insulation system, the consequences and possible diagnostic tools is given.

2.1. Insulation System

Typically, the main insulation of rotating high-voltage machines consists of mica tapes with a glass-fibre carrier. The layered mica tapes are resin impregnated, resulting in a PD-resistant insulation system. Outer corona protection (OCP) ensures equipotential bonding within the slot, while end corona protection (ECP) serves as electrical field grading at the slot exit. For GVPI machines the insulated coils are inserted in the laminated stator core before impregnation. Subsequently, the stator including the premounted coils is vacuum-pressure-impregnated and cured. The result is an adhesive bond between conductor, main insulation and laminated stator core. [1]

2.2. Thermomechanical Stress

During operation the temperature of the copper conductors increases e.g. due to Joule losses. With respect to the initial length L_0 the copper expands

according to

$$\Delta L = L_0 \cdot \alpha \cdot \Delta T, \quad (1)$$

where ΔL is the length expansion, α the coefficient of thermal expansion (CTE) and ΔT the temperature increase. While the stator temperature also increases, the temperature usually remains lower than the copper temperature. Accordingly, the total ΔT value differs between the stator core and the copper conductors. Additionally, the CTE varies for different materials. Both effects result in different thermal expansion of the copper conductor and the laminated stator core. Due to adhesion between conductor, main insulation and laminated stator core thermomechanical stress occurs within the main insulation. The occurring thermomechanical stress depends strongly on the operating mode and the manufacturer. Accordingly, no general statement can be made regarding at what length L_0 countermeasures need to be taken. If no countermeasures are taken, possible effects include crack formation at the slot exit, abrasion of the OCP near the slot exit or cooling channels and delamination in the main insulation (Fig. 1).

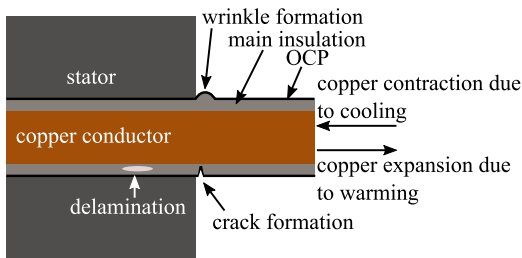


Fig. 1 – Possible effects of thermal cycling on GVPI coils according to [2]

The aforementioned delaminations can be subdivided into four categories, which are displayed in Fig. 2, depending on their position within the insulation [3].

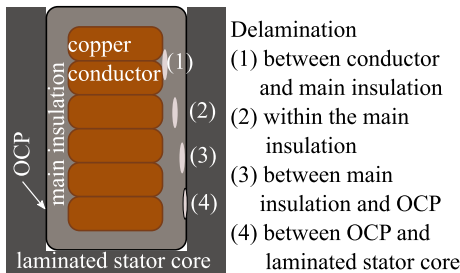


Fig. 2 – Categories of delamination possibly occurring due to thermomechanical stress

Generally, the area near the slot exit is regarded to be the most critical due to the increasing build up of thermomechanical stress as well as the sudden change in fixture when the coil exits the slot [4].

2.3. Diagnostic Tools

Based on the experience of [5]–[7] several diagnostic tools including capacitance, dielectric loss factor and PD measurements are worth considering for the detection of aforementioned symptoms of thermomechanical ageing.

It was found, that PD measurements allow conclusions on the insulation state after thermomechanical stress based on the charge value, the inception voltage and phase-resolved partial discharge patterns (PRPD) [5], [7]. Additionally, an increase in the dielectric loss factor as well as a decrease of the capacitance due to delamination is observed [5], [6].

2.3.1. Capacitance Measurement

While the capacitance of an intact insulation system consists of the capacitance value of named insulation system only, delaminations add lower partial capacitance values due to the reduced ϵ_r value. This results in a decrease of the overall capacitance of the insulation system. Due to the integral character of this measurement, no information on the number, localisation and shape of delaminations and voids can be gained. [8]

2.3.2. Dielectric Loss Factor Measurement

Dielectric loss factor measurements are used for integral detection of the dielectric losses of an insulation system. The sole value of the dielectric loss factor allows conclusions on the general condition of the insulation system including curing state and manufacturing quality. However, the electrical field dependent change of the dielectric loss factor, the dielectric loss factor tip up, allows to draw conclusions on the existence of voids and delaminations in the insulation system. [6]

Generally, the dielectric loss factor $\tan \delta$ comprises three components: conduction losses, polarization losses and ionization losses. The conduction and polarization losses are material-dependent and change only little with a change in the applied voltage and thus the electric field. The ionization losses however equal zero as long as no PDs occur. Once the PD inception voltage PDIV is reached a sharp increase in the ionization losses and thus the dielectric loss factor can be observed. Accordingly, the dielectric loss factor tip up $\Delta \tan \delta$

$$\Delta \tan \delta = \tan \delta_{\text{PD}} - \tan \delta_{\text{noPD}} \quad (2)$$

between one value $\tan \delta_{\text{noPD}}$ below and one above PD inception $\tan \delta_{\text{PD}}$ indicates whether voids or delaminations exist within the insulation system. [6] Due to the integral character of dielectric loss factor measurements, no information on the number, size and position of voids and delamination can be obtained. [6]

2.3.3. Partial Discharge Measurement

PD measurements have proven to be a powerful diagnostic tool due to the wide range of information that can be obtained. Aside from the PDIV, the number of impulses and the apparent charge can be evaluated.

Furthermore, PRPDs allow correlation with fault specific PRPDs. Based on the symmetry it can further be deduced, whether the fault is in contact with either conductor, grounded slot or neither. Nevertheless, PD measurements remain an integral diagnostic tool and thus do not allow the exact localisation of faults in small-scale specimens as described below. [5], [7]

3. Experimental

The experiments are conducted on test objects (sec. 3.1.), which undergo mechanical stress (sec. 3.2.1.) and subsequent electrical diagnosis (sec. 3.2.2.).

3.1. Test Objects

Insulated conductors are placed in a simple slot model to replicate the state of coils near the slot exit (Fig. 3).

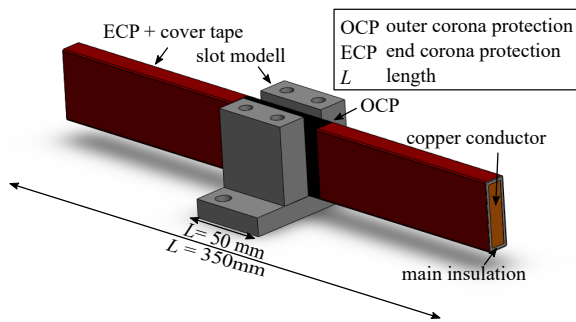


Fig. 3 – Specimen used for investigation

The conductor consists of a massive copper bar. The mica tape layers of the main insulation are machine-wound around the copper conductor. The insulation thickness corresponds to a rated voltage of $U_r = 11$ kV. Within the slot region OCP is applied. ECP tape is applied to achieve electrical field grading and avoid surface PDs in air at the sharp edges of the slot exit. Furthermore, cover tape is applied outside the slot region. The slot model consists of massive steel components mounted perpendicularly to replicate slot dimensions. The entire specimen consisting of conductor, insulation, OCP, ECP, cover tape and slot model undergoes a GVPI process, thus forming an adhesive system. After the GVPI process, three specimens are mechanically cut out of one bar. The investigation presents the results of a total number of five specimens, including specimens representing new-state conditions as well as specimens displaying signs of damage possibly due to specimen preparation.

3.2. Test Procedure and Setup

The test procedure consists of two phases: In phase one, the specimens are stressed mechanically to replicate longitudinal thermal expansion. Phase two occurs directly after phase one and comprises electrical measurements to evaluate whether the mechanical stress induces any faults in the insulation system and which diagnostic tool is most sensitive to detect the induced

faults. Both phases are repeated cyclically until the copper conductor tears out of the slot model irreversibly.

3.2.1. Mechanical stress

To replicate longitudinal thermal expansion of the copper conductor a compression-tension machine (Zwick/Roell Z050) displaces the conductor with a velocity of $v = 51.5 \mu\text{m s}^{-1}$ by applying force to a compression die the size of the copper conductor. The slot model is fixated resulting in a relative movement between conductor and slot model. The maximum displacement of the conductor increases with each stress level starting at $\Delta s_1 = 0.1$ mm with an increase of $\Delta s = 0.1$ mm per level (Fig. 4). Each stress level comprises one cycle.

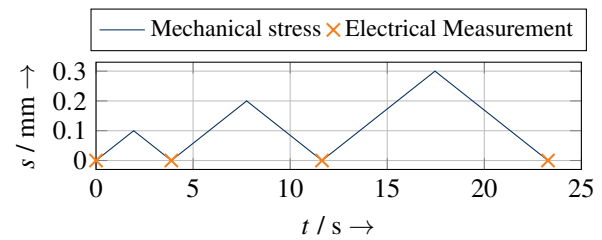


Fig. 4 – Stress and testing procedure

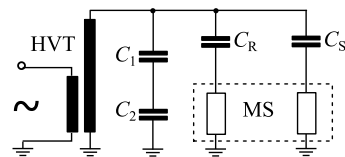
The maximum displacement is increased one more time after irreversible tear out of the slot model occurs, thus ensuring significant mechanical damage. After each stress level electrical measurements are conducted.

3.2.2. Electrical Measurement

For the electrical measurements two setups are used: one for dielectric loss factor and capacitance measurement, the other for PD measurements.

Dielectric Loss Factor and Capacitance Measurement

The setup for dielectric loss factor and capacitance measurements consists of a high-voltage transformer, a reference capacitance, a specimen and a measurement system (Omicron MI 600, Fig. 5).



HVT high-voltage transformer C_R reference capacitance
 C_1, C_2 capacitive measurement divider C_S specimen
 MS measurement system

Fig. 5 – Experimental setup for dielectric loss factor and capacitance measurement

One-minute measurements are conducted in 2.2kV intervals starting at $U_{RMS} = 2.2$ kV up to a maximum of $U_{RMS} = 13.2$ kV and a subsequent gradual reduction to $U_{RMS} = 2.2$ kV. The measured values are evaluated over a time span of approximately 50s per voltage level.

Partial Discharge Measurement

The PD measurement circuit consists of a high-voltage transformer, a blocking impedance ($L = 90\text{mH}$), a coupling capacitor ($C_c = 1\text{nF}$) and a capacitive voltage divider. A PD measurement system (Omicron MPD 600) records the PD signals transmitted via a measurement impedance (Fig. 6). The noise floor lies below $Q = 2\text{pC}$. The PDIV is determined for a threshold of $Q_{\text{thr}} = 5\text{pC}$ as the mean value of five cycles of voltage in- and decrease.

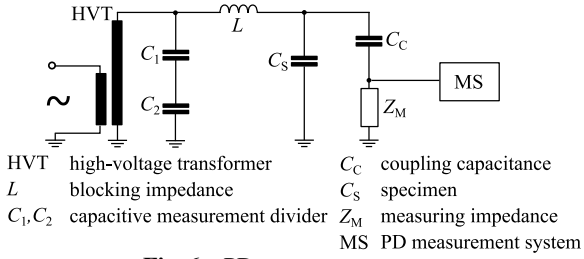


Fig. 6 – PD measurement setup

Charge and PRPD are determined from four-minute measurements at the same voltage levels as the capacitance measurement. The average charge is evaluated over a three-minute time span at 8.8kV measuring every 0.6s .

4. Results

The displacement at rupture varies for different specimens (S1-S5). For comparison between specimens, the applied displacement Δs is normalised to its maximum value s_{max} . This gives a relative push-out distance, ranging from zero, the unstressed condition to one, the maximum displacement.

4.1. Capacitance Measurements

At four out of five specimens the capacitance decreases between mint condition and rupture (Fig. 7).

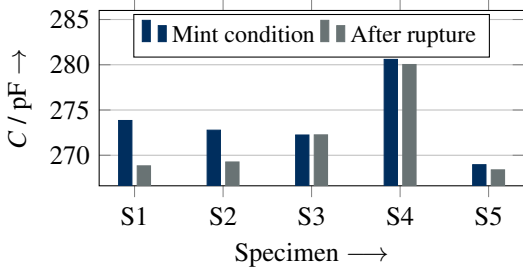


Fig. 7 – Measured capacitance of several specimens at 8.8kV

While the decrease for specimens S1 and S2 is apparent, the decrease for specimens S4 and S5 is negligible. The capacitance of specimen S3 remains approximately constant. Accordingly, the capacitance alone enables no reliable detection of rupture due to mechanical stress.

4.2. Dielectric Loss Factor Measurements

To evaluate the capability of dielectric loss factor measurements to detect the effects of thermomechanical

ageing, the dielectric loss factor values $\tan \delta_{U,i}$ for each stress level i are normalised to their respective start value at zero displacement $\tan \delta_{U,0}$, with U indicating the voltage level relative to U_r that was applied (3):

$$\Delta \tan \delta_U = \frac{\tan \delta_{U,i} - \tan \delta_{U,0}}{\tan \delta_{U,0}} \cdot 100\% \quad (3)$$

Evidently, the normalised dielectric loss factor increases noticeably once a first tear occurs and even further after rupture (Fig. 8). This phenomenon is more pronounced at lower voltage levels, indicating that PD activity and hence $\tan \delta$ at lower voltages increases due to mechanical damage, while the increase at higher voltages is negligible due to already increased PD occurrence. No significant $\tan \delta$ change before rupture can be observed. The deviations of the relative push-out distance originate in the different absolute push-out distance, which effects the normalised values and lead to different measurement intervals for each specimen.

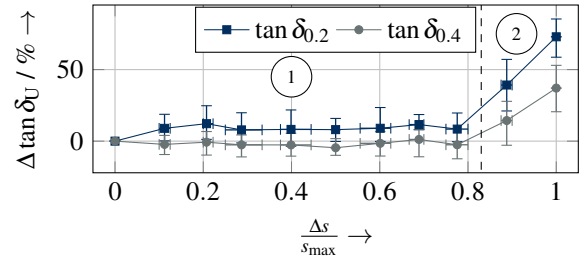


Fig. 8 – Mean value and absolute deviation of five specimens for $\Delta \tan \delta_U$ as a function of the relative push-out distance ①-before rupture ②-after rupture

4.3. Partial Discharge Measurements

Results of the PD measurements comprise values for the PDIV, the average charge Q_{AVG} and PRPD.

PD-inception voltage

PDIV measurements reveal a complex picture with a tendency of decreasing PDIV over increasing relative push-out distance (Fig. 9).

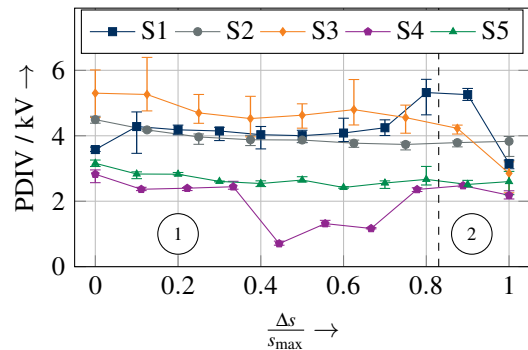


Fig. 9 – PDIV as a function of the relative push-out distance ①-before rupture ②-after rupture

Specimens S1 and S4 display significant changes in the PDIV before rupture, indicating partially reversible changes (elastic deformation) within the insulation

system due to mechanical stress even before rupture is mechanically detected. The values demonstrate that intrinsic changes can in- or decrease the PDIV of the respective insulation system during elastic deformation. Accordingly, PD-inception appears to be sensitive to insulation-immanent changes before rupture.

Average charge value

Specimens S1 to S5 vary significantly in their initial charge value most likely due to specimen preparation (Fig. 10, Fig. 11). The difference of the initial charge values coincides with different behaviours of the charge after mechanical stress. All three specimens with low charge values (S1, S2, S3, Fig. 10) display rather constant average charge values partially with a slight increase (S4, S5) until rupture.

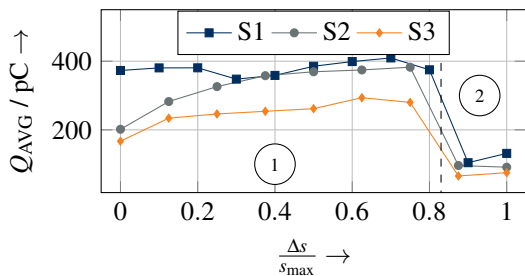


Fig. 10 – Q_{AVG} for specimens with low initial charge values
①-before rupture ②-after rupture

Once mechanical rupture occurs, the charge value decreases significantly. For this phenomenon is not fully understood, further investigations regarding the cause need to be conducted.

The behaviour of specimens with higher initial charge values is less consistent (Fig. 11). While specimen S4 displays a charge drop for the final value, no significant drop at rupture can be observed.

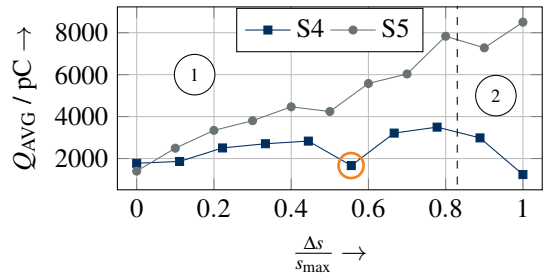


Fig. 11 – Q_{AVG} for specimens with high initial charge values
①-before rupture ②-after rupture

The striking low value at approximately $\frac{\Delta s}{s_{max}} \approx 0.55$ results from a time span of $t \approx 72$ hours between mechanical stress and electrical measurement, indicating that damage caused up to this point is reversible and changes with resting time. However, further investigations need to be conducted to verify this thesis. Specimen S5 displays no significant decrease in charge at all, but rather a constant increase, indicating expansion and multiplication of delaminations and cavities. The high initial charge values indicate delaminations and cavities in the initial state, thus forming a weak spot of the insulation system. Further mechanical stress possibly intensifies these weak spots, thus increasing the overall charge level. Depending on the extent of the delaminations, rupture possibly occurs at the respective weak spots, thus increasing the charge value even further.

Phase-Resolved Partial Discharge Patterns

Exemplary PRPD patterns confirm the findings of the average charge (Fig. 12). While the PRPDs for specimen S1 change negligibly between the initial state and $\frac{\Delta s}{s_{max}} = 0.5$, a significant increase of the overall PD activity can be observed for specimen S5. Specimen S1 displays typical rabbit ear patterns indicating voids, while

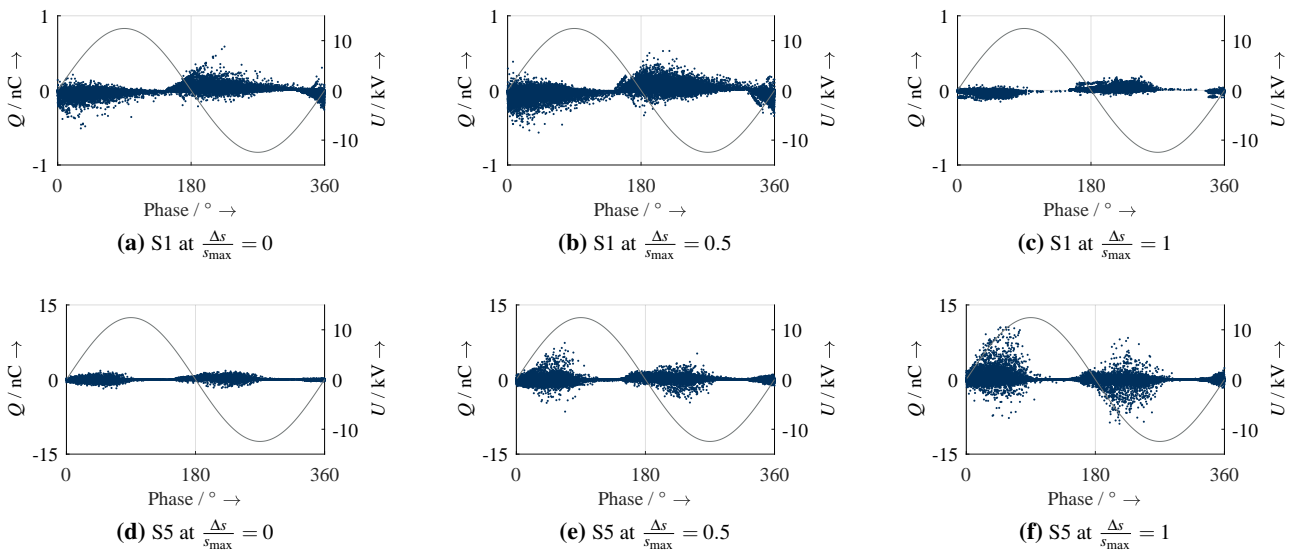


Fig. 12 – Development of PRPD for different relative push-out distances

nonetheless occurs at specimen S5, suggesting a different cause. Rupture at specimen S1 results in a significant decrease of the overall PD activity, whereas the PRPD of specimen S5 becomes further pronounced.

5. Discussion

It was shown, that the measured capacitance does not reliably correlate to the increasing mechanical stress, contrasting the findings in [6]. Nevertheless, the final rupture of the specimen usually leads to a capacitance decrease. The dielectric loss factor however detects progressing damage due to mechanical stress reliably with a significant increase at low voltages after rupture. The reason for this is most likely a lower PDIV once mechanical damage is introduced, since occurring PDs increase the $\tan \delta$. This concurs with the findings of [5] and [6], where an increase of the dielectric loss factor due to thermal cycling and thus thermomechanical ageing is observed. Nonetheless, no indication of the insulation condition before rupture is obtained, thus allowing only the detection of irreversible damage.

PD measurements give a reliable indication of intrinsic changes in the insulation system. Concurring with [7] it is found, that the PDIV is sensitive to mechanical rupture, displaying a noticeable decrease. The PDIV varies when the specimens are elastically deformed before rupturing. The displacement of the inner conductor can relieve the mechanical stress that is inherent due to the manufacturing process, but it can also introduce mechanical stress. This can lead to smaller or larger defect sizes and hence decreasing or increasing PD activity. According to [5] and [7], ageing results in a significant increase of the charge value, whereas this contribution shows that the behaviour can be twofold and strongly depends on the specimens initial condition:

1. Specimens with low initial charge values in this study exhibit a significant decrease of the charge values after rupture. The cause of this phenomenon requires further investigation.
2. Specimens with higher initial charge values coincide with the findings of [5] and [7], indicating that the applied stress increases the overall charge value suggesting an increase of void and delamination content even before mechanical rupture. The different behaviour is attributed to the significantly higher initial charge value, indicating considerable delamination or voids in the initial state, which are further aggravated by mechanical stress.

6. Conclusion

This paper presents the suitability of several diagnostic methods in detecting damages as a consequence of thermomechanical ageing. Typical damages are

replicated on small-scale test objects with an epoxy-mica insulation system by applying a push-out force up to rupture of the adhesive bond. The investigation indicates that dielectric loss factor measurements successfully detect irreversible mechanical rupture of the insulation system, whereas capacitance measurements fail to detect named rupture reliably. Thereagainst, PD measurements offer insight into electrically-effective changes in the insulation system even before mechanical rupture. While the PDIV indicates intrinsic changes, PRPD patterns allow further conclusions due to the specific shape of the PRPD. Accordingly, PD-measurements in combination with dielectric dissipation factor measurements make the analysis of damages due to thermomechanical ageing possible to a certain degree. The quality of the damage diagnosis is subjected to reproducibility of the specimens so that additional investigations are worthwhile. Additionally, the consequences of repetitive mechanical stress before and after rupture should be investigated to replicate the effects of several cycles of thermal expansion and contraction, thereby contributing to a better understanding of the insulation system of dynamically-operated long rotating machines.

References

- [1] G. C. Stone. *Electrical insulation for rotating machines: Design, evaluation, aging, testing, and repair*. 2nd Edition. Piscataway, NJ, USA: IEEE Wiley, 2014.
- [2] J. A. Nurse. "Modern global vacuum and pressure insulation systems for large high voltage machines". In: *1997 Electrical Electronics Insulation Conference and Electrical Manufacturing and Coil Winding Conference*. Piscataway, NJ, USA: IEEE, 1997.
- [3] M. Istad, M. Runde, and A. Nysveen. "A Review of Results From Thermal Cycling Tests of Hydrogenerator Stator Windings". In: *IEEE Transactions on Energy Conversion*. Vol. 3. 2011.
- [4] A. Cimino, C. Foelting, F. Jenau, and C. Staubach. "Analysis of localized dissipation factor measurements on the insulation system of mechanically aged generator stator bars". In: *Proceedings of the 2016 IEEE International Conference on Dielectrics*. IEEE, 2016.
- [5] M. Farahani, H. Borsi, E. Gockenbach, and M. Kaufhold. "Partial discharge and dissipation factor behavior of model insulating systems for high voltage rotating machines under different stresses". In: *IEEE Electrical Insulation Magazine*. Vol. 21. 2005.
- [6] M. Farahani, H. Borsi, and E. Gockenbach. "Study of Capacitance and Dissipation Factor Tip-Up to Evaluate the Condition of Insulating Systems for High Voltage Rotating Machines". In: *Electrical Engineering*. Vol. 89. 2007.
- [7] A. Cimino, F. Jenau, and C. Staubach. "Causes of cyclic mechanical aging and its detection in stator winding insulation systems". In: *IEEE Electrical Insulation Magazine*. Vol. 35. 2019.
- [8] A. K uchler. *Hochspannungstechnik: Grundlagen - Technologie - Anwendungen*. 4. Aufl. 2017. Springer Berlin Heidelberg, 2017.